# Shell Cross-Linked Nanoparticles Containing Hydrolytically Degradable, Crystalline Core Domains

**Qi Zhang, Edward E. Remsen,† and Karen L. Wooley***

*Contribution from the Department of Chemistry, Washington University, One Brookings Drive, St. Louis, Missouri 63130-4899*

*Received November 8, 1999*

**Abstract:** Shell cross-linked knedel-like nanoparticles (SCKs) possessing an amphiphilic core−shell morphology consisting of a cross-linked shell and a hydrolytically degradable, crystalline core domain were synthesized from poly(ϵ-caprolactone)-*b*-poly(acrylic acid) (PCL-*b*-PAA) amphiphilic diblock copolymers via a two-step process: self-assembly of PCL-*b*-PAA into polymer micelles followed by cross-linking of the hydrophilic shell layer via condensation reactions between the carboxylic acid functionalities of PAA and the amine groups of 2,2′-(ethylenedioxy)bis(ethylamine). PCL-*b*-PAA was prepared from the selective hydrolysis of a poly(ϵ-caprolactone)-*b*-poly(*tert*-butyl acrylate) (PCL-*b*-P*t*BA) precursor, which was synthesized by ring opening polymerization (ROP) of ϵ-caprolactone (ϵ-CL) followed by atom transfer radical polymerization (ATRP) of *tert*-butyl acrylate (*t*BA). Selective hydrolysis of the *tert*-butyl ester groups of the P*t*BA block by reaction with trimethylsilyl iodide (TMSI), followed by reaction with aqueous acid, gave PCL-*b*-PAA with nearly 100% conversion and minimal cleavage of the PCL chain segments. Alternatively, selective thermal deprotection of the *tert*-butyl esters was also performed. SCKs prepared from PCL-*b*-PAA formed globular nanoparticles when deposited from aqueous solution onto a mica surface at room temperature. The effects of copolymer composition and cross-linking extent on the properties of the SCKs were investigated by tapping-mode atomic force microscopy (AFM). The PCL core domains exhibited interesting crystallization and melting behaviors, in which the PCL melting transition temperature increased as the SCK core volume increased. This suggests that the lamellar thicknesses of PCL cores in larger SCKs are greater. The selective hydrolysis of the polyester (PCL) core domain in the presence of amide cross-links throughout the shell layer to yield nanocage structures was studied by $^1$H NMR and AFM. The degradation of PCL was monitored by $^1$H NMR, from the appearance of the resonance for sodium 6-hydroxyhexanoate under basic hydrolysis conditions. From AFM analysis for the nanoparticles adsorbed onto a mica surface, it was found that, under both acidic and basic hydrolysis conditions, the core-degraded nanocages formed broader structures with decreased height, in comparison with SCKs before core hydrolysis.

## Introduction

There has been a growing interest in the design and synthesis of polymer nanostructures with ever-increasing degrees of complexity and control over the composition and structure. In many cases, these materials are inspired from biological systems in design, construction, or properties, and application in biological or biomedical fields is promising.[1−5] As a mimic of globular proteins, synthetic nanoparticles having core−shell morphology have been prepared by the self-assembly of block copolymers, to afford polymer micelles, followed by intramicellar cross-linking. The cross-linking, which has been achieved by reactions performed within the core domain[6] or throughout the shell layer,[7−11] introduces covalent stabilization for the polymer micelles to reinforce the micellar architecture and result in high stability toward dilution and shear forces. Shell cross-linked micelles with hydrophilic core[12] and zwitterionic properties[13] have also been prepared recently. These materials are essentially single molecules of nanometer-scale dimensions. Therefore, they exhibit unique and robust character, which avoid the morphological changes that can occur for their supramolecular micellar precursors under environmental variations, such as changes in ionic strength,[14] solvent system,[15] and pH.[16] Additionally,

* To whom correspondence should be addressed. E-mail: KLWooley@artsci.wustl.edu. Phone: (314) 935-7136. Fax: (314) 935-9844 or -4481.
† Monsanto Co., 800 N. Lindbergh, St. Louis, MO 63167.

(1) Langer, R. *Nature* **1998**, *392*, 5.
(2) Kataoka, K. In *Controlled Drug Delivery: the Next Generation;* Park, K. E., Ed.; American Chemistry Society: Washington, DC, 1997; Chapter 4.
(3) Peracchia, M. T.; Gref, R.; Minamitake, Y.; Domb, A.; Lotan, N.; Langer, R. *J. Controlled Release* **1997**, *6*, 223.
(4) Domb, A. J.; Gref, R.; Minamitake, Y.; Peracchia, M. T.; Langer, R. S. Nanoparticles and microparticles of nonlinear hydrophilic−hydrophobic multiblock copolymers. WO Pat. 9503356, 1995.
(5) Zhang, L.; Eisenberg, A. *Science* **1995**, *268*, 1728.
(6) Henselwood, F.; Liu, G. *Macromolecules* **1997**, *30*, 488.
(7) Thurmond II, K. B.; Kowalewski, T.; Wooley, K. L. *J. Am. Chem. Soc.* **1996**, *118*, 7239.
(8) Thurmond, K. B., II; Kowalewski, T.; Wooley, K. L. *J. Am. Chem. Soc.* **1997**, *119*, 6656.
(9) Wooley, K. L. *Chem.—Eur. J.* **1997**, *3*, 1397.
(10) Huang, H.; Kowalewski, T.; Remsen, E. E.; Gertzmann, R.; Wooley, K. L. *J. Am. Chem. Soc.* **1997**, *119*, 11653.
(11) Huang, H.; Wooley, K. L.; Remsen, E. E. *Chem. Commun.* **1998**, 1415.
(12) Bütün, V.; Billingham, N. C.; Armes, S. P. *J. Am. Chem. Soc.* **1998**, *120*, 11818.
(13) Bütün, V.; Lowe, A. B.; Billingham, N. C.; Armes, S. P. *J. Am. Chem. Soc.* **1999**, *121*, 4288.
(14) Zhang, L.; Yu, K.; Eisenberg, A. *Science* **1996**, *272*, 1777.
(15) Yu, Y.; Eisenberg, A. *J. Am. Chem. Soc.* **1997**, *119*, 8383.
(16) Shen, H.; Zhang, L.; Eisenberg, A. *J. Am. Chem. Soc.* **1999**, *121*, 2728.

10.1021/ja993941o CCC: $19.00 
Published on Web 03/24/2000

variation over the core and shell composition and dimensions has been demonstrated, and the stability achieved through covalent cross-linking suggests that these nanostructures can serve in a capacity similar to that of micelles, for example, in the transport and delivery of guest molecules,[17−23] under particularly demanding conditions.

We have chosen to focus on shell cross-linked (SCK) polymer micelles to investigate the effect of the cross-linked membrane-like shell on the transport properties of guests to and from the core, while maintaining a mobile core domain. SCK nanoparticles have shown significant potential as water-miscible synthetic carriers or sequestrants.[24−26] Additionally, since stabilization is provided by binding together of the shell, the polymer chains that constitute the core can be degraded and extracted to leave hollow nanocage networks.[27,28] In the previous studies, nanocage-like structures were prepared by ozonolysis of polyisoprene core material. With the promise that SCKs and their resulting nanocages have demonstrated, their construction from hydrolytically degradable components is desirable for mild core removal and for potential biodegradability following utilization of the nanostructures. Biodegradable polyesters, such as poly($\epsilon$-caprolactone) (PCL), have been widely used as the matrixes for controlled drug release,[29−33] and PCL has now been incorporated into the core of SCKs containing a hydrogel shell of cross-linked poly(acrylic acid)/polyacrylamide. We report here the preparation and characterization of amphiphilic diblock copolymers of poly($\epsilon$-caprolactone) and poly(acrylic acid), their transformation to water-miscible nanoparticles, and their further modification to generate nanoscale cage-like membranes. Interesting findings related to the PCL crystalline phases restricted in nanodomains will also be discussed.

## Results and Discussion

The preparation of the core-degradable nanoparticles utilized a combination of self-assembly and covalent bond formation for the rapid production of stable structures. Therefore, the synthesis of amphiphilic diblock copolymers, poly($\epsilon$-caprolactone)-*b*-poly(acrylic acid), was followed by polymer micelle formation and then intramicellar cross-linking reactions between the polymer chains located within the hydrophilic peripheral domain of the polymer micelles.

**Scheme 1**

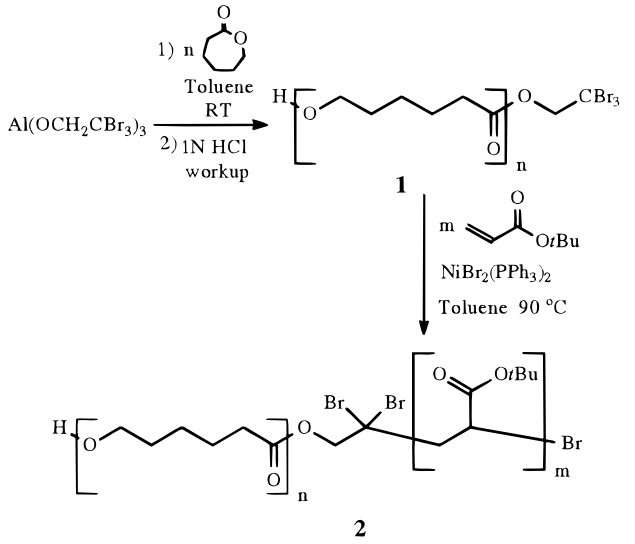


**Table 1.** Characterization Data of the Compositions, Molecular Weights, and Molecular Weight Distributions of PCL Macroinitiators and PCL$_n$-*b*-P*t*BA$_m$ Diblock Copolymers by $^1$H NMR and SEC

| polymer | $n^a$ | $m^b$ | $M_n$ ($^1$H NMR) | $M_n$ (SEC) | $M_w/M_n$ |
|---|---|---|---|---|---|
| **1** | 30 | 0 | 3 700 | 7 100 | 1.15 |
| **2a** | 30 | 9 | 4 900 | 9 600 | 1.18 |
| **2b** | 30 | 44 | 9 600 | 15 300 | 1.12 |
| **4** | 121 | 0 | 14 000 | 43 700 | 1.35 |
| **5a** | 121 | 8 | 15 200 | 44 500 | 1.32 |
| **5b** | 121 | 18 | 16 700 | 46 000 | 1.29 |
| **5c** | 121 | 158 | 34 300 | 61 000 | 1.41 |
| **5d** | 121 | 165 | 35 100 | 64 100 | 1.41 |

[a] Number of caprolactone repeating units in the PCL block according to $^1$H NMR end-group analysis. [b] Number of *t*BA repeating units in the P*t*BA block, determined by comparison of the intensity of the unique PCL protons resonating at 4.02 ppm to the intensity of the resonance from 2.1 to 2.3 ppm from overlapping PCL and P*t*BA protons, in the $^1$H NMR spectra.

Poly($\epsilon$-caprolactone)-*b*-poly(acrylic acid) (PCL-*b*-PAA) was prepared from the selective hydrolysis of poly($\epsilon$-caprolactone)-*b*-poly(*tert*-butyl acrylate) (PCL-*b*-P*t*BA), which was synthesized by ring opening polymerization (ROP) of $\epsilon$-caprolactone followed by atom transfer radical polymerization (ATRP) of *tert*-butyl acrylate (*t*BA).[34−37] Two synthetic routes were employed in the synthesis of PCL-*b*-P*t*BA copolymers. As illustrated in Scheme 1, the ROP of $\epsilon$-caprolactone ($\epsilon$-CL) initiated by Al(OCH$_2$CBr$_3$)$_3$ produced PCL, **1**, containing one hydroxy chain end and one tribromoethyl ester chain end. The unique alkyl tribromo group was then employed as the initiating species for the ATRP of *t*BA with the addition of NiBr$_2$(PPh$_3$)$_2$ as the catalyst, to afford PCL-*b*-P*t*BA **2a**,**b** (Scheme 1 and Table 1). Alternatively, ROP of $\epsilon$-CL by AlEt$_2$(O*i*Pr) placed an isopropyl ester at the initiated chain end, and the hydroxy chain

(17) Kim, S. Y.; Shin, I. G.; Lee, Y. M. *J. Controlled Release* **1998**, *56*, 197.
(18) Yokoyama, M.; Satoh, A.; Sakurai, Y.; Okano, T.; Matsumura, Y.; Kakizoe, T.; Kataoka, K. *J. Controlled Release* **1998**, *55*, 219.
(19) Chung, J. E.; Yokoyama, M.; Yamato, M.; Aoyagi, T.; Sakurai, Y.; Okano, T. *J. Controlled Release* **1999**, *62*, 115.
(20) Jones, M. C.; Leroux, J. C. *Eur. J. Pharm. Biopharm.* **1999**, *48*, 101.
(21) Oh, I.; Lee, K.; Kwon, H.-Y.; Lee, Y.-B.; Shin, S.-C.; Cho, C.-S.; Kim, C.-K. *Int. J. Pharm.* **1999**, *181*, 107.
(22) Kim, S. Y.; Shin, I. G.; Lee, Y. M. *Biomaterials* **1999**, *20*, 1033.
(23) Gan, Z.; Jim, T. F.; Li, M.; Yuer, Z.; Wang, S.; Wu, C. *Macromolecules* **1999**, *32*, 590.
(24) Thurmond, K. B., II; Wooley, K. L. *ACS Symposium Series on Materials for Controlled Release Applications*; McCulloch, I., Shalaby, S. W., Ed.; American Chemical Society: Washington, DC, 1998; p 165.
(25) Baugher, A. H.; Goetz, J. M.; McDowell, L. M.; Huang, H.; Wooley, K. L.; Schaefer, J. *Biophys. J.* **1998**, *75*, 2574.
(26) Thurmond, K. B., II; Remsen, E. E.; Kowalewski, T.; Wooley, K. L. *Nucleic Acids Res.* **1999**, *27*, 2966.
(27) Huang, H.; Remsen, E. E.; Kowalewski, T.; Wooley, K. L. *J. Am. Chem. Soc.* **1999**, *121*, 3805.
(28) Ding, J.; Liu, G. *J. Phys. Chem. B* **1998**, *102*, 6107.
(29) Gebelein, C. G.; Mirza, T.; Chapman, M. *Polym. Mater. Sci. Eng.* **1987**, *57*, 413.
(30) Wang, P. Y. *J. Biomed. Mater. Res.* **1989**, *23*, 91.
(31) Bei, J.-Z.; Li, J.-M.; Wang, Z.-F.; Le, J.-C.; Wang, S.-G. *Polym. Adv. Technol.* **1997**, *8*, 693.
(32) Ha, J.-H.; Kim, S.-H.; Han, S.-Y.; Sung, Y.-K.; Lee, Y.-M.; Kang, I.-K.; Cho, C.-S. *J. Controlled Release* **1997**, *49*, 253.
(33) Barakat, I.; Dubois, P.; Grandfils, C.; Jérôme, R. *J. Polym. Sci., Part A: Polym. Chem.* **1999**, *37*, 2401.
(34) Matyjaszewski, K.; Patten, T. E.; Xia, J. *J. Am. Chem. Soc.* **1997**, *119*, 674.
(35) Mecerreyes, D.; Moineau, G.; Dubois, P.; Jérôme, R.; Hedrick, J. L.; Hawker, C. J.; Malmström, E. E.; Trollsås, M. *Angew. Chem., Int. Ed.* **1998**, *37*, 1274.
(36) Hawker, C. J.; Hedrick, J. L.; Malmström, E. E.; Trollsås, M.; Mecerreyes, D.; Moineau, G.; Dubois, P.; Jérôme, R. *Macromolecules* **1998**, *31*, 213.
(37) Moineau, G.; Minet, M.; Dubois, P.; Teyssie, P.; Senninger, T.; Jérôme, R. *Macromolecules* **1999**, *32*, 27.

**Scheme 2**

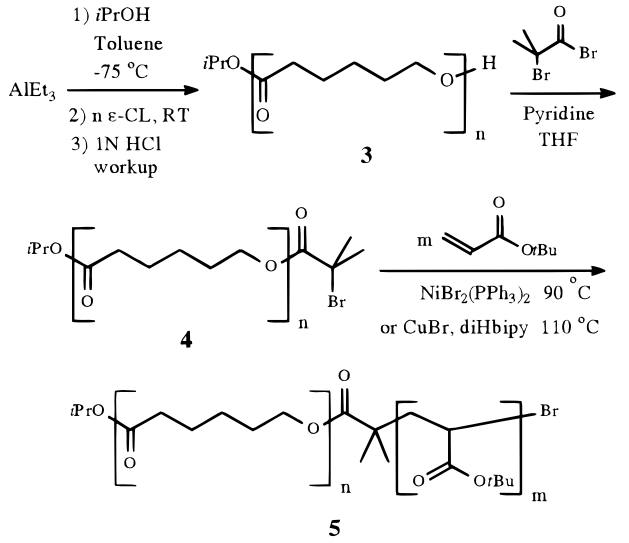


end of this PCL **3** was then modified by reaction with 2-bromoisobutyryl bromide to incorporate an alkyl bromide functionality and yield the PCL macroinitiator **4**. ATRP of *t*BA from **4** in the presence of $NiBr_2(PPh_3)_2$ or CuBr catalyst then gave PCL-*b*-P*t*BA diblock copolymers **5a**−**d** (Scheme 2 and Table 1). It was found that $NiBr_2(PPh_3)_2$ was a more effective catalyst with tribromoethylterminated PCL macroinitiator, **1**, whereas CuBr performed best with 2-bromoisobutyl-terminated PCL macroinitiator, **4**.

The compositions and molecular weight distributions of the PCL macroinitiators and PCL-*b*-P*t*BA diblock copolymers were characterized by $^1$H NMR and size exclusion chromatography (SEC) (Table 1). The significant differences between the molecular weights determined by $^1$H NMR and those from SEC analysis were likely due to the SEC instrument calibration by polystyrene standards. Therefore, SEC was mainly used to monitor the growth profiles and molecular weight distributions for the diblock copolymers, while the compositions and molecular weights of the PCL and PCL-*b*-P*t*BA samples were determined by $^1$H NMR end group analysis, with further confirmation by elemental analysis (EA) and thermogravimetric analysis (TGA). The relative and overall lengths of the PCL and P*t*BA blocks were varied to investigate the effect of copolymer composition on the properties of the SCK nanoparticles.

Selective deprotection of the *tert*-butyl acrylate groups by reaction with TMSI[38,39] in $CH_2Cl_2$ followed by hydrolysis using 0.1 N HCl then gave the PCL-*b*-PAA amphiphilic diblock copolymers from the PCL-*b*-P*t*BA precursors (Scheme 3). Model hydrolysis reactions using mixtures of PCL and P*t*BA homopolymers were first performed to optimize the reaction conditions for selective removal of the *tert*-butyl esters while avoiding breakdown of the PCL chains (Table 2). $^1$H NMR showed that the resonance for the *tert*-butyl ester groups of P*t*BA completely disappeared after reaction with TMSI for 1 h at room temperature, and SEC analysis of the mixture demonstrated that PCL was only slightly cleaved under these conditions. The times that were allowed for reaction of the PCL-*b*-P*t*BA copolymers with TMSI at room temperature were, therefore, limited to be within 1 h (Table 3), and removal of the *tert*-butyl ester groups was confirmed by the complete disappearance of the *tert*-butyl

(38) Jung, M. E.; Lyster, M. A. *J. Am. Chem. Soc.* **1977**, *99*, 968.
(39) Smith, C. K.; Liu, G. *Macromolecules* **1996**, *29*, 2060.

**Scheme 3**

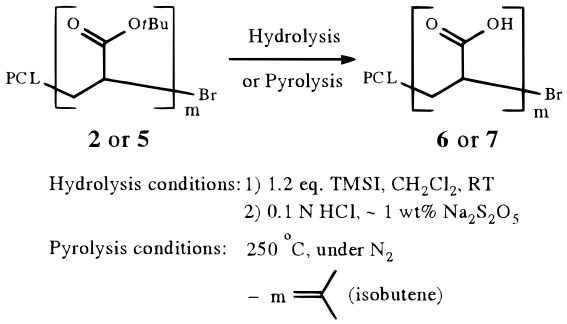


**Table 2.** Data from Model Reactions Using Blends of PCL and P*t*BA Homopolymers To Determine Reaction Conditions for Selective Deprotection of the *tert*-Butyl Ester Groups by Reaction with TMSI/0.1 N HCl, While Limiting Cleavage of the PCL

| hydrolysis time | $M_n$ (GPC) of PCL[a] | $M_w/M_n$ | resonance of *t*Bu groups[b] |
|---|---|---|---|
| 0 | 39 800 | 1.32 | |
| 1 | 35 100 | 1.48 | not detectable |
| 2 | 19 000 | 1.76 | not detectable |

[a] After the hydrolysis reaction sequence, the remaining PCL homopolymer was precipitated in cold methanol and GPC analysis was performed. [b] The methanol phase was then concentrated and a $^1$H NMR spectrum was obtained in a mixed solvent system of THF-$d_8$ and $D_2O$ (10:1) to determine the extent of hydrolysis of *t*Bu ester. No resonance for *tert*-butyl groups was detectable in the spectra of the PAA-containing supernatant or the PCL precipitate ($CDCl_3$).

**Table 3.** Compositional Data for the PCL-*b*-PAA Copolymers

| $PCL_n$-*b*-$PAA_m$ | $n$[a] | $m$ | PCL-*b*-P*t*BA precursor | hydrolysis time (min) | resonance for *t*Bu ester groups[b] |
|---|---|---|---|---|---|
| **6a** | 30 | 9 | **2a** | 40 | not detectable |
| **6b** | 30 | 44 | **2b** | 60 | not detectable |
| **7a** | 121 | 8 | **5a** | 50 | not detectable |
| **7b** | 121 | 18 | **5b** | 40 | not detectable |
| **7c** | 105 | 158 | **5c** | 40 | not detectable |
| **7d** | 105 | 165 | **5d** | 50 | not detectable |

[a] Number of caprolactone repeat units of PCL block after hydrolysis, determined by comparison of the intensity of the unique PCL protons resonating at 4.02 ppm to the intensity of the resonance from 2.2 to 2.5 ppm from overlapping PCL and P*t*BA protons, in the $^1$H NMR spectra. [b] Determined from $^1$H NMR (THF-$d_8$/$D_2O$, 10:1) as the complete disappearance of the *tert*-butyl resonance at 1.42 ppm.

$^1$H resonance at 1.42 ppm. By controlling the hydrolysis time, *tert*-butyl ester side groups were removed selectively while leaving the PCL backbone essentially intact. However, the PCL backbones of **7c** and **7d** were partially degraded, which was presumably because of the relatively high concentration of TMSI required for complete deprotection of the longer P*t*BA chain segments in the last two reactions. The compositions of the PCL-*b*-PAA copolymers were determined by comparison of the intensity of the unique PCL protons resonating at 4.02 ppm to the intensity of the resonance from 2.2 to 2.5 ppm from overlapping PCL and PAA protons, in the $^1$H NMR spectra collected using a solvent mixture of THF-$d_8$ and $D_2O$ (v/v = 10/1).

The thermal stability of PCL-*b*-P*t*BA was studied by TGA. By comparing the thermal degradation of the diblocks with the results for PCL, P*t*BA, and PAA homopolymers, the first weight loss at ca. 250 °C was attributed to the thermal decomposition of the *tert*-butyl ester groups and the release of isobutene. The theoretical weight loss due to the loss of isobutene, calculated from the composition of each PCL-*b*-P*t*BA diblock copolymer, correlated well with the experimental data (Table 4), which

**Table 4.** TGA Data (25−500 °C, 10 °C/min under $N_2$ Flow) for the Pyrolytic Deprotection of P*t*BA and PCL-*b*-P*t*BA[a]

| polymer | % wt loss (isobutene) calcd[b] | % wt loss (isobutene) exptl[c] | $T_d$ (°C)[d] |
|---|---|---|---|
| P*t*BA | 43.8 | 42.5 | 215 |
| **2a** | 10.4 | 10.2 | 186 |
| **2b** | 26.4 | 26.8 | 201 |
| **5a** | 3.0 | 2.4 | 208 |
| **5b** | 6.2 | 5.9 | 231 |
| **5c** | 25.9 | 25.2 | 243 |

[a] The decomposition temperatures ($T_d$) for the *tert*-butyl esters to produce isobutene are given. For reference, the $T_d$ of PCL is 379 °C. [b] The percentage weight loss from pyrolytic deprotection of the *tert*-butyl esters is calculated from the composition of the polymer; for $PCL_n$-*b*-P*t*$BA_m$, calcd wt % loss = $[m(MW_{isobutene})/(M_n \text{ of polymer})] \times 100\%$. [c] The percentage weight loss determined by TGA was the difference of the weight percentage between the onset and offset deprotection temperatures. [d] The deprotection temperature was determined as the onset temperature of the first weight loss.

suggested that the *tert*-butyl esters were quantitatively removed. Considering the fact that the deprotection temperatures for the *tert*-butyl ester side groups of the P*t*BA blocks (ca. 250 °C) were far below the decomposition temperature of PCL (ca. 400 °C), it was possible to achieve the removal of *tert*-butyl ester groups by pyrolysis below 300 °C, without affecting the PCL block. This served as an alternative to the TMSI/0.1 N HCl chemical deprotection approach (Scheme 3). Therefore, selective pyrolysis in the TGA instrument was performed on a 10 mg sample of **5c** with heating to 275 °C under $N_2$ flow, and the *tert*-butyl ester pyrolysis was observed by $^1$H NMR in a solvent mixture of THF-$d_8$ and $D_2O$ (v/v = 10/1). Disappearance of the resonance for the *tert*-butyl protons at 1.42 ppm and a downfield shift of the resonance of the methine proton from 2.1−2.3 ppm (C***H***COO*t*Bu) to 2.2−2.5 ppm (C***H***COOH) were characteristic of the transformation of **5c** to **7e**. The composition of **7e** was determined to be $PCL_{120}$-*b*-$PAA_{158}$ by comparison of the intensities for the PAA and PCL protons giving an overlapping resonance of 2.2−2.5 ppm (C***H***COOH and C***H***$_2$$(CH_2)_4$OCO), with the unique PCL protons resonating at 4.02 ppm ($(CH_2)_4$C***H***$_2$OCO) in the $^1$H NMR spectra, which confirmed that the PCL backbone was essentially intact after thermal treatment. In contrast to the slight cleavage of the PCL backbone of **7c**, $PCL_{105}$-*b*-$PAA_{158}$, which occurred by the TMSI/0.1 N HCl chemical method, this selective pyrolysis method actually appears to be better, and study on larger scales is ongoing.

The SCKs were then prepared by the two-step assembly and covalent stabilization procedure, employing the PCL-*b*-PAA materials as the amphiphilic diblock copolymers capable of supramolecular organization (Scheme 4). Polymer micelles were formed by first dissolving PCL-*b*-PAA in a solvent mixture of THF/$H_2O$, 20:1, and then gradually adding water as a nonsolvent for PCL. Usually, a one-to-one volume ratio of $H_2O$ to THF was reached before the THF was removed by dialysis against deionized water. Stabilization of the polymer micelles was then achieved through formation of the SCK nanoparticles by cross-linking the hydrophilic shell layer via condensation reactions between the carboxylic acid functionalities of PAA and the amine functional groups of 2,2′-(ethylenedioxy)bis(ethylamine) in the presence of 1-(3-dimethylaminopropyl)-3-ethylcarbodiimide methiodide as the coupling reagent (Scheme 4), following the procedure described previously.[10] PCL-*b*-PAA copolymers with different overall and relative lengths of the hydrophobic and hydrophilic block segments were used to prepare SCKs of different dimensions[8] (Table 5). The percentages of cross-linking

**Scheme 4**

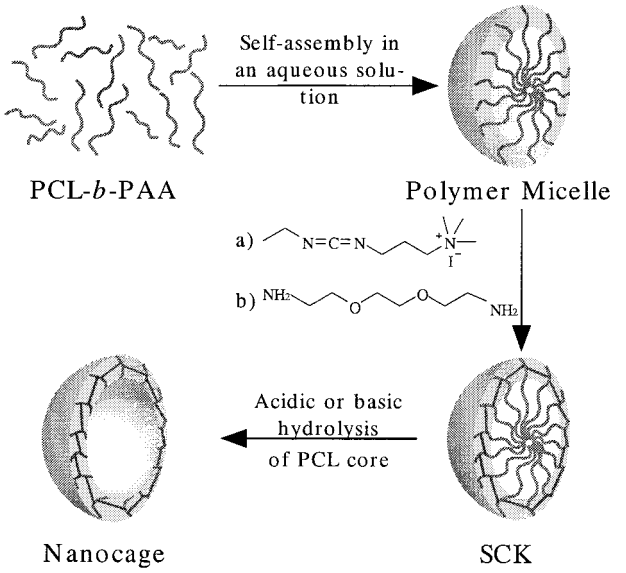


**Table 5.** Characterization Data for the SCKs

| SCK | diblock polymer | percent cross-linking (%)[a] | $H_{av}$[b] (nm) | $D_{av}$[c] (nm) | $D_h$[d] (nm) | $T_m$[e] (°C) | $T_g$[e] (°C) |
|---|---|---|---|---|---|---|---|
| **8** | **6b** | 50 | 6 ± 1 | 40 ± 6 | | | |
| **9** | **7b** | 50 | 20 ± 1 | 109 ± 15 | | | |
| **10** | **7b** | 25 | 16 ± 2 | 83 ± 8 | 100 ± 1 | | |
| **11** | **7b** | 50 | 17 ± 3 | 105 ± 9 | 99 ± 1 | | |
| **12** | **7b** | 100 | 18 ± 3 | 172 ± 13 | | 58 | −62 |
| **13**[f] | **7c** | 100 | 8 ± 1 | 43 ± 5 | 44 ± 4 | 48 | −67 |
| | | | 15 ± 2 | 103 ± 16 | 255 ± 50 | 56 | −50 |
| **14** | **7d** | 50 | 10 ± 1 | 45 ± 6 | | 53 | −68 |

[a] The percentage of cross-linking was based on the stoichiometric ratio of amine and carboxylic acid functionalities of the cross-linker and PAA block segments, respectively. These values represent the maximum theoretical amount of cross-linking that can take place. [b] Average heights of SCK nanoparticles deposited from aqueous solution onto a mica surface and allowed to dry in vacuo, measured by tapping-mode AFM. [c] Average diameters of SCK nanoparticles deposited from aqueous solution onto a mica surface and allowed to dry in vacuo, measured by tapping-mode AFM. [d] Hydrodynamic diameters of SCKs in aqueous solution, determined by dynamic light scattering. [e] The temperatures of melting transitions ($T_m$) and glass transitions ($T_g$) of the PCL core were measured by DSC as the peak maximum for $T_m$ and the midpoint of the inflection tangent for $T_g$, and are average values of three runs upon the fourth through sixth heating scans. [f] Sample **13** contained a bimodal distribution of SCK nanoparticle sizes, as observed by AFM and DLS, and these gave two distinct $T_m$ values.

given in Table 5 are the stoichiometries of amine functional groups of the cross-linker added to the carboxylic acid groups present; however, this is merely the maximum amount of amidation that can occur, rather than an accurate description of the true extent of cross-linking. In amide formation, the diamine can undergo reaction with two separate PAA chain segments to yield a cross-link, coupling to the same chain to form "loops", or attachment by only monoaddition to leave a dangling amine. Although the extent of cross-linking is not absolutely known, this terminology is used for descriptive purposes. Extensive labeling strategies and NMR experiments are ongoing to accurately determine the degree of cross-linking.

The size and shape of the polymer micelles and SCK nanoparticles were characterized by tapping-mode atomic force microscopy (AFM), by measurement and comparison of the height and diameter values. As expected, cross-linking of the shell domain of the polymer micelles assisted in the maintenance of their three-dimensional structure, and enhanced their stability.

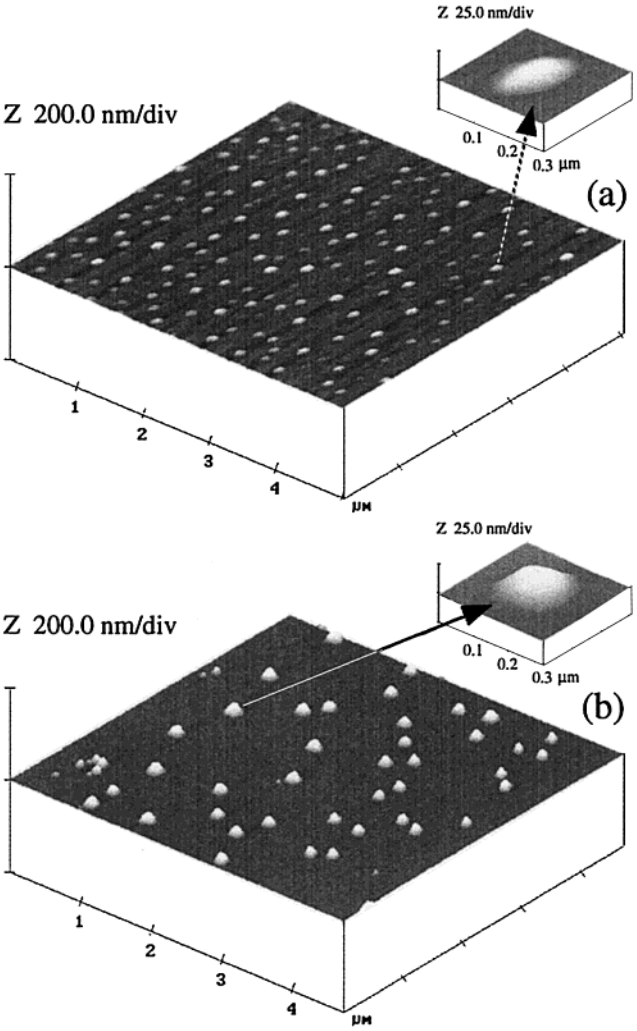


**Figure 1.** Tapping-mode AFM images of (a) polymer micelles and (b) 50% cross-linked SCK nanoparticles (SCK **9**), each prepared from **7b** in an aqueous solution and then deposited onto mica and allowed to dry in vacuo. The enlargements show the images of one micelle and SCK particle.

For example, upon adsorption on the mica surface, the polymer micelles of **7b** form a flat circular structure with an average height of 5 nm (Figure 1a), whereas 50% cross-linked SCKs (SCK **9**) prepared from the same micelle solution appeared as particles with an average height of 20 nm (Figure 1b).

To study the effect of cross-linking extents on the structures of the SCKs, SCKs **10**−**12** were prepared from the same stock solution of micelles composed of **7b**, with cross-linking percentages of 25%, 50%, and 100%, respectively (Figure 2).[40] The differences among the heights of SCKs **10**−**12**, measured in the solid state by AFM, were within experimental deviations, as listed in Table 5. The solutions of SCKs **10** and **11** were also analyzed by dynamic light scattering (DLS), and the hydrodynamic diameters ($D_h$) were 100 ± 1 and 99 ± 1 nm, respectively. The insensitivity of the sizes of SCKs to cross-linking extents can be explained by the short length of the PAA block of **7b** and the low molecular weight of the cross-linker

(40) Note: SCKs **10**−**12** were prepared from a micelle solution different from that used to prepare SCK **9**. It has been shown that micelle size depends on many factors, including diblock concentration and micelle formation time.[8] However, in these cases, the dimensions of the SCKs were very similar, e.g., comparison of **9** and **11**, when prepared from the same diblock copolymer and with the same cross-linking extent, even though the micelle samples used to prepare SCKs **10** and **11** and SCK **9** were from different stock solutions.

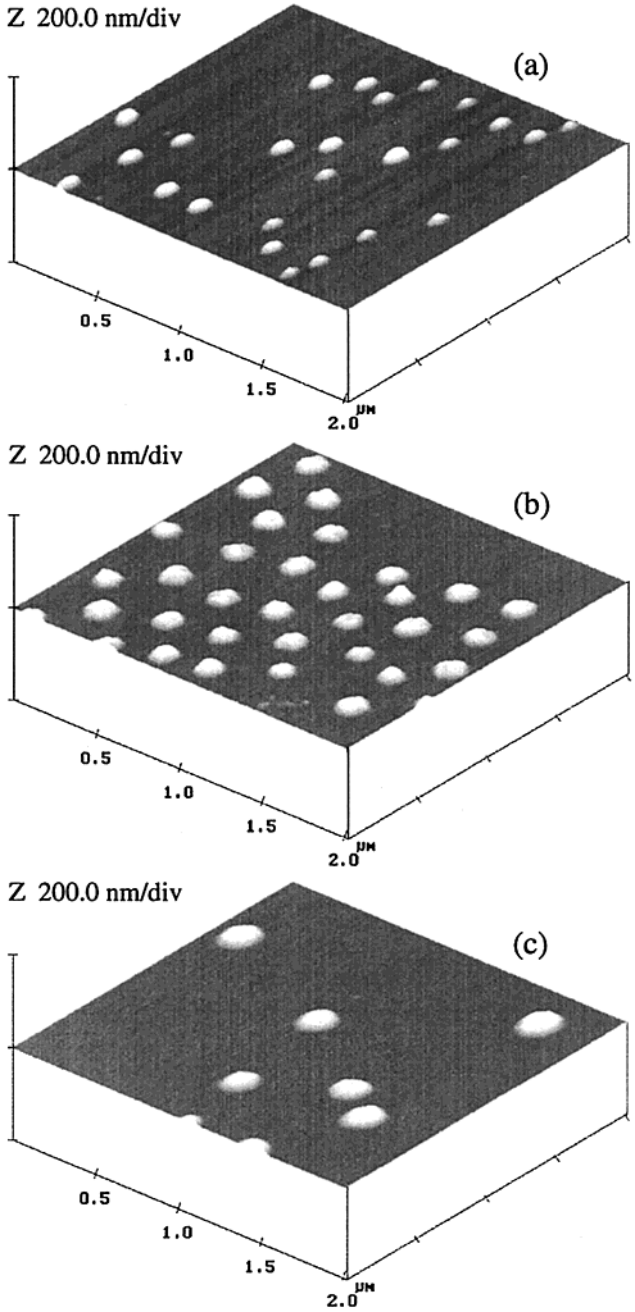


**Figure 2.** Tapping-mode AFM images of SCKs (deposited from aqueous solution onto mica and allowed to dry in vacuo) prepared from **7b** with differing degrees of shell cross-linking: (a) SCK **10**, 25% cross-linked; (b) SCK **11**, 50% cross-linked; (c) SCK **12**, 100% cross-linked.

used in this study, which add little volume to the SCK upon incorporation of the cross-linker. Moreover, the PCL is a crystalline polymer, and it is believed that the crystallization of the PCL core upon nucleation to form the polymer micelles offers substantial reinforcement to the nanostructures and controls their shape and size. Since each of the SCKs **10**−**12** originated from micelles of **7b**, this suggests that the cross-links do not disrupt a preformed crystalline assembly. The formation of platelike crystalline lamellae is further supported by the discrepancy between the AFM height and diameters measured by AFM and DLS. Additional discussion of the PCL crystallinity is included in the description of thermal transitions found below. Importantly, these results indicate that cross-linking extents of less than 25% of the carboxylic acid functional groups achieve reinforcement of the micelle structure, while

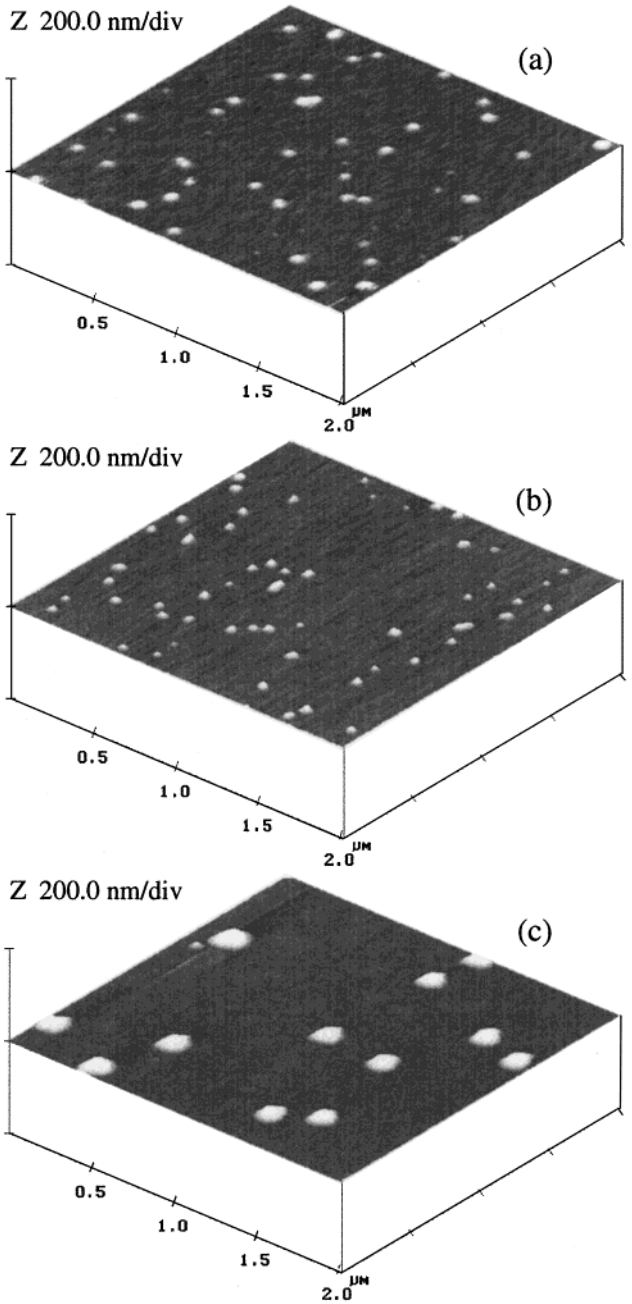


**Figure 3.** Tapping-mode AFM images of SCKs (deposited from aqueous solution onto mica and allowed to dry in vacuo) prepared from different diblock copolymers: (a) SCK **8**; (b) SCK **14**; (c) SCK **9**.

leaving more than 75% of the carboxylic acid groups available to function as active sites for pH-sensitive hydrogel materials or as reactive sites for further functionalization.

The influence of the diblock copolymer composition upon the SCK dimensions was also investigated (Figure 3). As the overall length of the diblock copolymer was increased while maintaining the relative lengths for the PCL and PAA blocks (**6b** vs **7d**), the height of SCKs increased modestly from $6 \pm 1$ to $10 \pm 1$ nm (**8** vs **14**). In comparison, alteration of the relative hydrophobic to hydrophilic content for the diblock copolymers had dramatic effects on the size of the SCKs, because of increased polymer chain aggregation numbers in polymer micelles[5] and SCKs,[41] as the hydrophobic/hydrophilic ratio increased. For example, **7b** had roughly the same PCL length as **7d**, but a much shorter PAA block. As a result, the height of SCK **9** was $20 \pm 1$ nm, in comparison to the $10 \pm 1$ nm height found for SCK **14**, prepared from **7b** and **7d**, respectively.

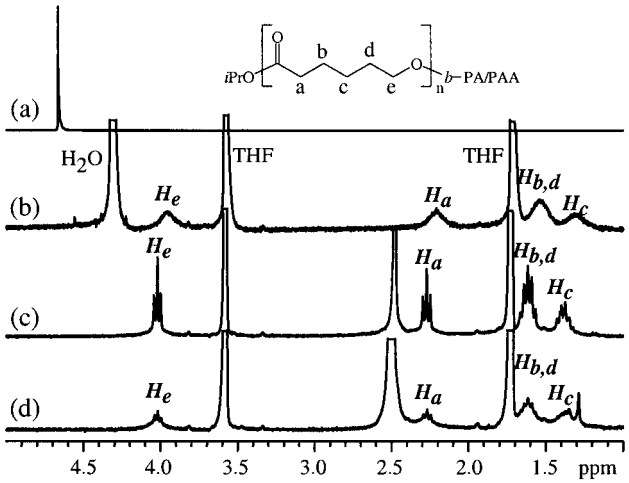


**Figure 4.** $^1$H NMR spectra of SCK **12** suspended in (a) $D_2O$, (b) $D_2O$/THF-$d_8$, 1:2, and (c) THF-$d_8$ with $CH_2Cl_2$ as an internal reference. Spectrum d was collected upon the supernatant of (c), after most SCKs had precipitated. The ratios of PCL to $CH_2Cl_2$ protons resonating at 4.02 ($H_e$, C***H***$_2$OCO) and 5.50 (C***H***$_2$Cl$_2$) ppm in $^1$H NMR were 4:1 in (c) and 1:1 in (d).

Lyophilized samples of the SCKs were easily redispersed in water and many organic solvents. However, the cross-linked shell prevented these nanoparticles from "truly" dissolving in a solvent, which made it challenging to characterize the compositions of the SCKs by solution-state NMR. For example, when SCK **12** was dispersed in $D_2O$ (Figure 4a), nothing but the resonance of the solvent peak could be observed. However, with the addition of THF-$d_8$, the resonance of the PCL appeared (Figure 4b), which could be explained by diffusion of THF-$d_8$ into the PCL core to swell and solvate the un-cross-linked PCL chains.[42] Meanwhile, from the preparation of **4** (Scheme 2), it was found that only 90% of the hydroxyl terminal groups of PCL were functionalized by the reaction with 2-bromoisobutyryl bromide. The presence of a small amount of PCL homopolymer (**3**) in **5a**−**d** was observed by the appearance of a small shoulder at the same retention volume as for **3** in the SEC traces of **5a**−**5d**. Since it was possible that the PCL resonance observed in Figure 4b was partially due to contamination by PCL homopolymers in SCK **12**, SCK **12** was dispersed in pure THF-$d_8$, with $CH_2Cl_2$ added as an internal reference (Figure 4c). Well-resolved resonances were observed for the PCL protons in this case, and the molar ratio of PCL to $CH_2Cl_2$ was determined to be 4:1. The SCKs were then allowed to precipitate over 2 days in the sealed NMR tube, and the molar ratio of PCL to $CH_2Cl_2$ decreased to 1:1 in the supernatant (Figure 4d). These results suggest that at least 75% of the intensity of the PCL resonance in Figure 4c originated from covalently attached chains in the core of the SCKs. Since not all SCKs precipitated, the detected amount of PCL in the supernatant (25% of the PCL core) was higher than the amount of homopolymer contamination in **4** (10%). Similar results were collected for SCK **13**, and when $CDCl_3$ was used as the solvent (in this case, the SCKs were of lower density and partitioned to the upper $CDCl_3$ layer, rather than precipitating).

The presence of the PCL homopolymer contaminant actually proved useful in generating SCKs having partially extracted

(41) Remsen, E. E.; Thurmond, K. B., II; Wooley, K. L. *Macromolecules* **1999**, *32*, 3685.

(42) Tuzar et al. have studied the swelling of non-cross-linked polymer micelle cores by NMR: Kriz, J.; Masar, B.; Pospisil, H.; Plestil, J.; Tuzar, Z.; Kiselev, M. A. *Macromolecules* **1996**, *29*, 7853.

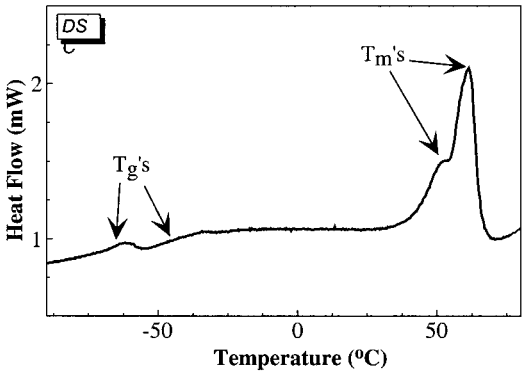


**Figure 5.** DSC characterization (10 °C/min) of SCK **13**, having a bimodal size distribution, illustrates the two melting transitions for PCL core domains.

cores,[43] and in monitoring the permeability of the cross-linked shell. Although PCL homopolymer was observed by SEC from the point of initial addition of THF and the amount of released PCL homopolymer increased steadily throughout a 24 h period of time, no accurate fit to the data has yet been possible. Further experiments to study the release behavior as a function of entrapped guest size and shape and the SCK shell thickness and cross-linking density are in progress.

Characterization of lyophilized samples of SCKs using DSC gave interesting findings related to the crystallization properties of the PCL core domains (Table 5). For SCKs consisting of PCL-*b*-PAAs with similar PCL block lengths, particles of smaller size (SCK **14**, average height by AFM of 10 ± 1 nm) exhibited a melting transition ($T_m$) at 53 °C, while the $T_m$ for particles of larger size (SCK **12**, average height by AFM of 18 ± 3 nm) was observed at 56 °C. In one particular sample (SCK **13**) that had a bimodal distribution of particle sizes (8 ± 1 and 15 ± 2 nm, average heights by AFM), two melting transitions were observed (48 and 56 °C) (Table 5 and Figure 5). The crystallization and melting behaviors of PCL have been extensively studied,[44−51] and it has been established that crystallization of PCL occurs by the spontaneous formation of folded chain structures within a lamellar lattice.[52] However, the movement of PCL chains in the SCK systems was restricted within the nanometer-scale core domain by being covalently bound to the internal wall of the cross-linked shell. It is conceivable to assume that the PCL lamellar thickness increases with increasing core volume, provided by SCKs of larger dimensions, which led to increased melting transition temperatures for the PCL core domains of the larger SCKs. The formation of platelike lamellae, driven by crystallization of the PCL core domains, is supported by the shapes of the SCKs, in which they are observed by AFM as having significantly greater

(43) Liu et al. have utilized the intentional entrapment of homopolymer chains into the core of core-cross-linked nanoparticles, followed by extraction of the homopolymer to produce nanoporous cores: Henselwood, F.; Liu, G. *Macromolecules* **1998**, *31*, 4213.

(44) Rim, P. B.; Runt, J. P. *Macromolecules* **1983**, *16*, 762.

(45) Goulet, L.; Prud'Homme, R. E. *J. Polym. Sci., Part B: Polym. Phys.* **1990**, *28*, 2329.

(46) De Juana, R.; Cortazar, M. *Macromolecules* **1993**, *26*, 1170.

(47) Vazquez-Torres, H.; Cruz-Ramos, C. A. *J. Appl. Polym. Sci.* **1994**, *54*, 1141.

(48) Vanneste, M.; Groeninckx, G.; Reynaers, H. *Polymer* **1997**, *38*, 4407.

(49) Nojima, S.; Kuroda, M.; Sasaki, S. *Polym. J.* **1997**, *29*, 642.

(50) Sanchis, A.; Prolongo, M. G.; Salom, C.; Masegosa, R. M. *J. Polym. Sci., Part B: Polym. Phys.* **1998**, *36*, 95.

(51) Nojima, S.; Kikuchi, N.; Rohadi, A.; Tanimoto, S.; Sasaki, S. *Macromolecules* **1999**, *32*, 3727.

(52) Rodriguez, F. *Principles of Polymer Systems*, 4th ed.; Taylor & Francis: Washington, DC, 1996; Chapter 3.

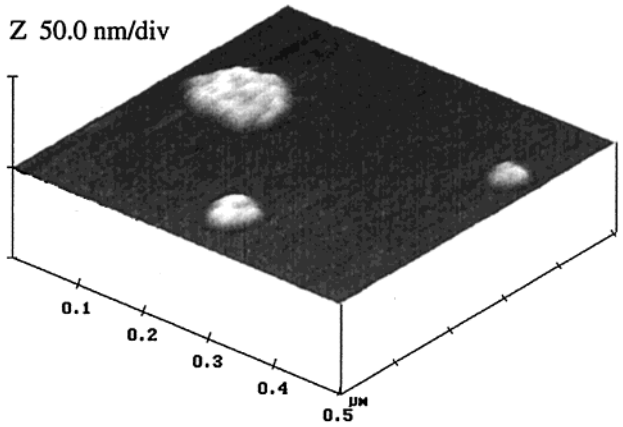


**Figure 6.** Tapping-mode AFM image of SCK **8** after hydrolysis under acidic conditions (2 M HCl, 70 °C, 15 h) (deposited from aqueous solution onto mica and allowed to dry in vacuo). The average height of SCKs after hydrolysis was 4 ± 1 nm.

diameters (widths) than heights (thicknesses) (Table 5). Moreover, DLS measurements gave hydrodynamic diameters that were in agreement with the AFM diameters, supporting the presence of a crystalline lamellar structure in solution as well. Further investigations of the crystallization behavior of PCL core domains within these unique nanostructured materials are in progress.

Because the amide functionalities of the shell cross-links are of higher stability than the ester linkages of the PCL core toward hydrolysis under both acidic and basic conditions, selective hydrolysis of the polyester core domain in the presence of the amide cross-links was accomplished (Scheme 4). Hydrolysis of SCK **8** by reaction with HCl (ca. 2 M) in an aqueous solution was first performed. The changes in the size and shape of SCKs upon core hydrolysis to yield hollow nanocages were studied using AFM. Evidence that some part of the SCK structure was hydrolyzed was provided by the decreased height of SCK **8** (from 6 to 4 nm). However, the aggregation of SCKs after hydrolysis (Figure 6) limited the ability to accurately evaluate these materials.

Therefore, degradation of the PCL core under basic conditions was then performed on SCK **14**. First, the hydrolysis of *N*-methylacetamide at increasing pH in $D_2O$ was studied by $^1H$ NMR as a model system to search for an optimized condition that allowed for the maximum hydrolysis rate of the polyester core domain without cleavage of the amide cross-links in the shell (Figure 7). It was found that *N*-methylacetamide was quite stable up to pH 12, and only 2% hydrolysis was observed after 14 days. With the acrylamide-type cross-links within the shell of the SCKs being sterically more hindered than *N*-methylacetamide, the hydrolysis of SCK **14** was performed at pH 12 for 14 days. The appearance of the small-molecule degradation product, sodium 6-hydroxyhexanoate, was monitored by $^1H$ NMR, with $D_2O$ as the solvent. In addition, decreased intensities for the proton resonances due to the PCL were observed by NMR analysis using THF-$d_8$ solvent. AFM characterization of SCK **14** after the hydrolysis under basic conditions displayed similar results as had been observed for the core removal under acidic conditions, in which flattened and broadened structures were observed on the mica surface (Figure 8). The average height of SCK **14** decreased from 10 ± 1 to 6 ± 1 nm and the average diameter increased from 45 ± 6 to 123 ± 16 nm upon core degradation and extraction. However, in this case, no aggregation was observed and each particle existed as a cross-linked membrane nanocage-like structure, which was presum-

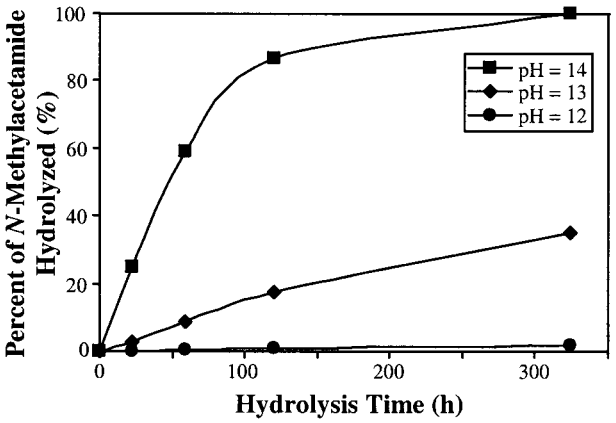


**Figure 7.** The percentage of *N*-methylacetamide hydrolyzed in $D_2O$ over time under different pH conditions was evaluated by $^1H$ NMR, from the integration ratio of the protons of *N*-methylacetamide and the hydrolysis product, methylamine.

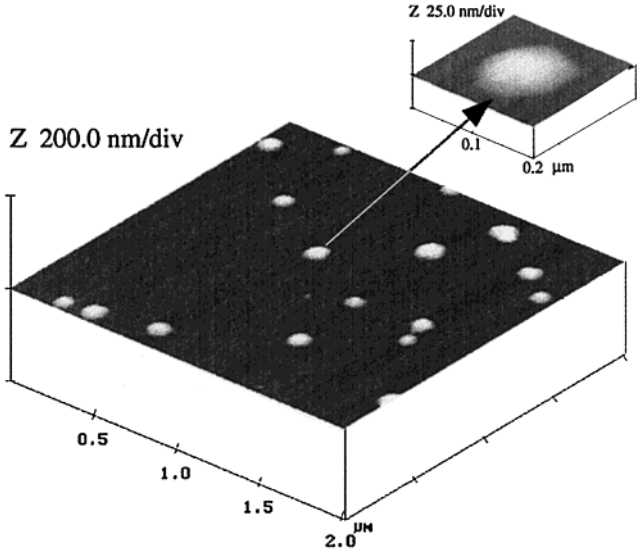


**Figure 8.** Tapping-mode AFM image of SCK **14** after hydrolysis under basic conditions (pH 12, room temperature, 14 days) (deposited from aqueous solution onto mica and allowed to dry in vacuo). The average height of the SCKs after hydrolysis was $6 \pm 1$ nm.

ably a three-dimensional expanded sphere in solution that collapsed on the mica surface to be observed in the dry state by AFM as a flattened, circular image, without any evidence for massive rupture of the cross-linked shell.

## Conclusions

Water-miscible nanoparticles possessing an amphiphilic core−shell morphology and a degradable core domain have been prepared from PCL-*b*-PAA via a two-step process: self-assembly of PCL-*b*-PAA to form polymer micelles in an aqueous solution and then cross-linking of the PAA shell layer through amidation chemistry. The overall synthetic approach to these SCK nanoparticles is versatile to allow for modification of the shell and core compositions, and thus tailoring of the properties and function, independently, from their surface, throughout their shell, across their interface, and into their core domains. The covalent cross-links provide for structural stability to maintain the amphiphilic core−shell morphology. The polyester core, which is encapsulated within the cross-linked hydrogel shell, is hydrolytically degradable, and the degradation product is biocompatible. Further modifications of the chemical composition and architecture of the SCKs are in progress.

The crystallization of the PCL core may contribute to the size and shape of these unique nanostructured materials, while dispersed in solution or deposited on solid substrates, and this is being further investigated by AFM and scattering techniques, combined with annealing studies of the micellar precursors and SCK nanomaterials. The findings on the dependence of the melting behavior of PCL core domains on the size of SCKs demonstrate that SCKs might serve as a potential system for fundamental studies involving the behavior of confined crystalline polymers, and they may lead to the organization of such restricted crystalline phases.

We are currently taking advantage of the unique degradable core domain to synthesize hollow SCK nanoparticles that are expected to allow for high guest loading or to exhibit unusual properties. The degradability of the PCL core could also be used to enhance the release of encapsulated hydrophobic guests or to provide for degradation of the SCK materials in the body or the environment after they have performed their function.

## Experimental Section

**Measurements.** IR spectra of samples were obtained on a Mattson Polaris spectrometer as KBr pellets. $^1H$ NMR spectra of solutions were recorded on a Varian Gemini 300 MHz spectrometer with the solvent proton resonance used as reference. $^{13}C$ NMR spectra were recorded at 75.4 MHz as solutions on a Varian Gemini 300 MHz spectrometer with the solvent carbon signal as reference.

SEC was conducted on a Hewlett-Packard series 1050 HPLC with a Hewlett-Packard 1047A refractive index detector. Data analysis was done by Viscotek (Houston, TX) Trisec GPC Software, v. 2.70. Two 5 $\mu$m Polymer Laboratories PL gel columns (300 × 7.7 mm) connected in the order of increasing pore size (500 Å, mixed bed E) were used. The eluent was THF distilled over $CaH_2$.

Glass transition temperatures and melting transition temperatures were measured by differential scanning calorimetry (DSC) on a Perkin-Elmer DSC-4 differential scanning calorimeter with heating rates of 10 °C/min. The $T_g$ was taken as the midpoint of the inflection tangent, and $T_m$ was taken as the temperature at the peak maximum, upon the third or subsequent heating scan. TGA was performed on a Perkin-Elmer TGS-2 thermogravimetric analyzer. For both DSC and TGA, the Perkin-Elmer instruments were upgraded with Instrument Specialists, Inc. (Antioch, IL) temperature program interface-PE, and data were acquired and analyzed using TA-PC software v. 2.11 (Instrument Specialists, Inc.).

Samples for AFM imaging were prepared by placing a 1.0 $\mu$L drop of polymer micelle or SCK solutions (typical concentration about 0.05 mg/mL) on freshly cleaved mica (Ruby clear mica, New York Mica Co.) and allowing it to dry in the air and then further dry in vacuo for 1−2 h. AFM imaging was performed using a Nanoscope IIIa system (Digital Instruments, Santa Barbara, CA) equipped with a J-type vertical engage piezoelectric scanner and operated in tapping mode in air. In tapping-mode imaging, the cantilever is oscillated above the surface at a frequency close to its resonance frequency and touches the sample surface intermittently at the peak of each oscillation cycle. The decrease in cantilever oscillation amplitude due to intermittent contacts is used as a control signal for a feedback loop to track the surface topography. Throughout this study, tapping-mode imaging was carried out with standard etched silicon probes ($l = 128$ $\mu$m, spring constant ~50 N/m, resonance frequency ~330 kHz) and cantilever oscillation amplitudes of about 10 nm. A typical value for the set point (the ratio of damped to free oscillation amplitudes) was 0.95. The typical raw signal corresponding to cantilever oscillation was ca. 1.0 V. Typical scan frequencies were between 0.5 and 2.0 Hz, depending on scan fields, which varied from 10 $\mu$m × 10 $\mu$m to 500 nm × 500 nm. The SCK diameters were taken as the heights of the SCK nanoparticles, which were measured by the bearing analysis procedure, using the Nanoscope III software package. Distributions of heights of the SCK nanoparticles were obtained from individual measurements performed on ~100 particles. The average diameters ($D_{av}$) were determined from measure-

ments performed on ~50 particles without correction of the effects for the silicon tip diameter (ca. 15−20 nm).

The size distribution for the SCKs in solution was determined by DLS. The DLS instrumentation was a Brookhaven Instruments Co. (Holtsville, NY) system consisting of a model BI-200SM goniometer, a model EMI-9865 photomultiplier, and a model BI-9000AT digital correlator. Incident light was provided by a model 95-2 Ar ion laser (Lexel Corp., Palo Alto, CA) operated at 514.5 nm. All measurements were made at 20 ± 1 °C. Prior to analysis, solutions were centrifuged in a model 5414 microfuge (Brinkman Inst. Co., Westbury, NY) for 4 min to sediment dust particles. Scattered light was collected at a fixed angle of 90°. The digital correlator was operated with 522 channels, a dual sampling time of 100 ns, a 5 $\mu$s ratio channel spacing, and a duration of 3 min. A photomultiplier aperture of 200 $\mu$m was used, and the incident laser intensity was adjusted to obtain a photon counting rate of 200 kcps. Only measurements in which measured and calculated baselines of the intensity autocorrelation function agreed to within 0.1% were used to calculate the particle size. The calculation of the particle size distribution and distribution averages was performed with the ISDA software package (Brookhaven Instruments Co., Holtsville, NY), which employed single-exponential fitting, cumulants analysis, and non-negatively constrained least-squares particle size distribution analysis routines.

**Materials.** 2,2,2-Tribromoethanol (97%), aluminum isopropoxide (99.99+%), $NiBr_2(PPh_3)_2$ (99%), CuBr (99.995%), 2,2′-bipyridine (99%), 1-bromohexane (98%), LDA (1.0 M in THF), triethylaluminum (1.0 M in hexane), 2-bromoisobutyryl bromide (97%), trimethylsilyl iodide (99%), 2,2′-(ethylenedioxy)bis(ethylamine), 1-(3-dimethylaminopropyl)-3-ethylcarbodiimide methiodide, and *N*-methylacetamide (99+%) were purchased from Aldrich and used as received. Toluene (HPLC grade, Aldrich) was dried by heating at reflux over calcium hydride and then distilled from sodium/benzophenone ketyl prior to polymerization. THF (HPLC grade, inhibitor free, Aldrich) was dried over calcium hydride and distilled from sodium/benzophenone ketyl. Dichloromethane was distilled from $CaH_2$. *t*BA, 2-propanol, and $\epsilon$-CL were dried over $CaH_2$ for 24 h at room temperature and vacuum transferred prior to polymerization. Spectra/Por Membranes (MWCO 3600, 6800, and 12000−14000) used for dialysis were obtained from Spectrum Medical Industries, Inc. (Laguna Hills, CA).

**General Procedure for the Preparation of Poly($\epsilon$-caprolactone)-*block*-poly(*tert*-butyl acrylate).** The diblock copolymers were prepared by ROP of $\epsilon$-caprolactone followed by ATRP of *tert*-butyl acrylate. The tribromoethoxy-terminated poly($\epsilon$-caprolactone) macroinitiator (**1**) and the hydroxyl-terminated PCL (**3**) were synthesized on a double manifold connected to high-vacuum line ($10^{-4}$ mmHg) and argon (99.9995%), following the procedure reported elsewhere.[36,53] **4** was then prepared from the hydroxyl-terminated PCL (**3**) by the reaction with 2-bromoisobutyryl bromide.[37] The yield of the functionalization was 90% determined by comparing the integration ratio of the two different chain ends, $(CH_3)_2CHOCO$ and $(CH_3)_2CBrCOO$, of **4**. The polymerization of *t*BA was accomplished on a double manifold connected to a vacuum line ($10^{-2}$ mmHg) and $N_2$ (UHP, 99.99%) line. In a typical ATRP experiment, the poly($\epsilon$-caprolactone) macroinitiator (**1** or **4**) (1 g, dried in vacuo), catalyst $NiBr_2(PPh_3)_2$[37] or CuBr[34] (0.01 equiv in comparison to *t*BA), and diHbipy (2.2 equiv in comparison to CuBr) were introduced into a previously dried Schlenck flask filled with nitrogen. A cycle of evacuation under vacuum and backfilling with nitrogen was repeated three times to remove oxygen. To the Schlenck flask were added toluene and *t*BA via a gastight syringe, and the mixture was degassed three times by freeze−pump−thaw cycles. The polymerization was performed under nitrogen flow at 90 ± 2 °C for 42 h (with $NiBr_2(PPh_3)_2$ catalyst) or at 110 ± 2 °C for 19 h (with CuBr catalyst). The polymers formed were then dissolved in THF and passed through a short alumina column to remove the catalysts. The diblock copolymers were recovered by precipitation into a cold 10:1 (v/v) methanol/water mixture and dried in vacuo at room temperature. The molecular weight distribution ($M_w/M_n$) of PCL-*b*-P*t*BA was determined by SEC and the numbers of $\epsilon$-CL repeating units (*n*) vs *t*BA repeating units (*m*) were determined by $^1$H NMR analysis. Six PCL-*b*-P*t*BA copolymers were prepared according to two series: for **2a**,**b**, the length of the PCL block was held constant ($M_n$ = 3700, $M_w/M_n$ = 1.15), while the degree of polymerization of the P*t*BA block was varied as either 9 or 44; for **5a**−**d**, the length of the PCL block ($M_n$ = 13 800, $M_w/M_n$ = 1.32) was held constant, while the degree of polymerization of the P*t*BA block was varied as 8, 18, 158, and 165. The P*t*BA block length was controlled primarily by the concentration of the polymerization mixture. IR (KBr pellets): 2960, 2940, 2867, 1729, 1458, 1395, 1368, 1250, 1154, 1108, 1045, 962, 847, 752 cm$^{-1}$. $^1$H NMR ($CDCl_3$): $\delta$ 1.2−1.9 [br, C***H***$_2$CH(COO*t*Bu)], 1.40 [m, CO(CH$_2$)$_2$C***H***$_2$(CH$_2$)$_2$O], 1.42 [s, CH$_2$-CHCOOC(C***H***$_3$)$_3$], 1.61 [m, COCH$_2$C***H***$_2$CH$_2$C***H***$_2$CH$_2$O], 2.1−2.3 [br, CH$_2$C***H***(COO*t*Bu)], 2.28 [t, $J$ = 6.0 Hz, COC***H***$_2$(CH$_2$)$_4$O], 4.02 [t, $J$ = 6.0 Hz, CO(CH$_2$)$_4$C***H***$_2$O)] ppm. $^{13}$C NMR ($CDCl_3$): $\delta$ 24.6 [CO-(CH$_2$)$_2$***C***H$_2$(CH$_2$)$_2$O], 25.5 [COCH$_2$***C***H$_2$(CH$_2$)$_3$O], 28.0 [***C***H$_2$CH-(COO*t*Bu)], 28.1 [CH$_2$CHCOOC(***C***H$_3$)$_3$], 28.3 [CO(CH$_2$)$_3$***C***H$_2$CH$_2$O], 34.1 [CO***C***H$_2$(CH$_2$)$_4$O], 37.4−42.2 [br, CH$_2$***C***H(COO*t*Bu)], 64.1 [CO-(CH$_2$)$_4$***C***H$_2$O], 80.2 [CH$_2$CHCOO***C***(CH$_3$)$_3$], 173.3 [***C***O(CH$_2$)$_5$O], 173.8 [CH$_2$CH***C***OO*t*Bu] ppm.

**Poly($\epsilon$-caprolactone)-*block*-poly(*tert*-butyl acrylate) (2a).** $NiBr_2(PPh_3)_2$ (0.10 g, 0.14 mmol) was used as the catalyst for the ATRP of *t*BA (2 mL, 10 mmol) upon macroinitiator **1** (1 g, 0.3 mmol) in toluene (2 mL). $n$ = 30, $m$ = 9, and $M_n$ = 4900 (by $^1$H NMR). $M_w/M_n$ = 1.18 (by SEC). Anal. Calcd for $C_{245}H_{411}O_{79}Br_3$: C, 60.54; H, 8.54. Found: C, 60.78; H, 8.73. TGA in $N_2$: 25−200 °C, 10% mass loss; 200−350 °C, 8% mass loss; 350−500 °C, 80% mass loss.

**Poly($\epsilon$-caprolactone)-*block*-poly(*tert*-butyl acrylate) (2b).** $NiBr_2(PPh_3)_2$ (0.12 g, 0.16 mmol) was used as the catalyst for the ATRP of *t*BA (2 mL, 10 mmol) upon macroinitiator **1** (1 g, 0.3 mmol) in toluene (1 mL). $n$ = 30, $m$ = 44, and $M_n$ = 9600 (by $^1$H NMR). $M_w/M_n$ = 1.12 (by SEC). Anal. Calcd for $C_{490}H_{831}O_{148}Br_3$: C, 62.96; H, 8.98. Found: C, 63.01; H, 8.83. TGA in $N_2$: 25−220 °C, 27% mass loss; 220−380 °C, 20% mass loss; 380−500 °C, 48% mass loss.

**Poly($\epsilon$-caprolactone)-*block*-poly(*tert*-butyl acrylate) (5a).** $NiBr_2(PPh_3)_2$ (0.05 g, 0.07 mmol) was used as the catalyst for the ATRP of *t*BA (2 mL, 10 mmol) upon macroinitiator **4** (0.9 g, 0.06 mmol) in toluene (10 mL). $n$ = 121, $m$ = 8, and $M_n$ = 15 000 (by $^1$H NMR). $M_w/M_n$ = 1.32 (by SEC). Anal. Calcd for $C_{789}H_{1319}O_{260}Br$: C, 62.98; H, 8.85. Found: C, 62.84; H, 8.82. TGA in $N_2$: 25−350 °C, 5% mass loss; 350−500 °C, 93% mass loss.

**Poly($\epsilon$-caprolactone)-*block*-poly(*tert*-butyl acrylate) (5b).** CuBr (0.0075 g, 0.052 mmol) and 4,4′-di-*n*-heptyl-2,2′-bipyridine (0.04 g, 0.1 mmol) were used as the catalyst for the ATRP of *t*BA (1 mL, 5 mmol) upon macroinitiator **4** (0.7 g, 0.05 mmol) in toluene (3.5 mL). $n$ = 121, $m$ = 18, and $M_n$ = 16 300 (by $^1$H NMR). $M_w/M_n$ = 1.29 (by SEC). Anal. Calcd for $C_{859}H_{1439}O_{280}Br$: C, 63.19; H, 8.90. Found: C, 63.01; H, 8.70. TGA in $N_2$: 25−250 °C, 6% mass loss; 250−365 °C, 4% mass loss; 365−500 °C, 88% mass loss.

**Poly($\epsilon$-caprolactone)-*block*-poly(*tert*-butyl acrylate) (5c).** CuBr (0.033 g, 0.23 mmol) and 4,4′-di-*n*-heptyl-2,2′-bipyridine (0.17 g, 0.48 mmol) were used as the catalyst for the ATRP of *t*BA (2 mL, 10 mmol) upon macroinitiator **4** (0.8 g, 0.06 mmol) in toluene (2 mL). $n$ = 121, $m$ = 158, and $M_n$ = 34 300 (by $^1$H NMR). $M_w/M_n$ = 1.41 (by SEC). DSC: $T_g$ = −61 °C, and $T_m$ = 57 °C for the PCL block. Anal. Calcd for $C_{1839}H_{3119}O_{560}Br$: C, 64.45; H, 9.19. Found: C, 64.28; H, 9.15. TGA in $N_2$: 25−255 °C, 25% mass loss; 255−380 °C, 18% mass loss; 380−500 °C, 51% mass loss.

**Poly($\epsilon$-caprolactone)-*block*-poly(*tert*-butyl acrylate) (5d).** CuBr (0.033 g, 0.23 mmol) and 4,4′-di-*n*-heptyl-2,2′-bipyridine (0.17 g, 0.48 mmol) were used as the catalyst for the ATRP of *t*BA (2 mL, 10 mmol) upon macroinitiator **4** (0.8 g, 0.06 mmol) in toluene (1.7 mL). $n$ = 121, $m$ = 165, and $M_n$ = 35 100 (by $^1$H NMR). $M_w/M_n$ = 1.41 (by SEC).

**General Procedure for the Preparation of Poly($\epsilon$-caprolactone)-*block*-poly(acrylic acid).** In a typical experiment, PCL-*b*-P*t*BA (ca. 1 g) was dissolved in dry dichloromethane (ca. 10 mL) in a previously flame-dried round-bottom flask connected to the $N_2$ line. To the solution was then added TMSI (1.2 equiv in comparison to *tert*-butyl ester groups), and the reaction mixture was stirred under nitrogen for 40−60 min before the solvent and excess TMSI were removed under reduced pressure. The resulting polymer was dissolved in THF. To the

(53) Jacobs, C.; Dubois, P.; Jérôme, R.; Teyssie, P. *Macromolecules* **1991**, *24,* 3027.

polymer solution was added dropwise 0.1 N HCl solution containing ca. 1 wt % $Na_2S_2O_5$. The mixture was stirred for 2 h, and then dialyzed against deionized water for 2 days to remove the salt and other byproducts. PCL-*b*-PAA was recovered by lyophilization (yield >95%). The numbers of $\epsilon$-CL repeating units ($n$) and acrylic acid repeating units ($m$) were determined by $^1$H NMR analysis. IR (KBr pellets): 3400−2700, 2960, 2860, 1724, 1451, 1421, 1295, 1246, 1191, 1149, 1106, 1044, 961, 842 cm$^{-1}$. $^1$H NMR (THF-$d_8$/$D_2O$ = 10/1): $\delta$ 1.37 [m, $CO(CH_2)_2CH_2(CH_2)_2O$], 1.5−2.0 [br, $CH_2CH(COOH)$], 1.61 [m, $COCH_2CH_2CH_2CH_2CH_2O$], 2.27 [t, $J$ = 6.0 Hz, $COCH_2(CH_2)_4O$], 2.2−2.5 [br, $CH_2CH(COOH)$], 4.02 [t, $J$ = 6.0 Hz, $CO(CH_2)_4CH_2O$] ppm. $^{13}$C NMR (THF-$d_8$/$D_2O$ = 10/1): $\delta$ 25.2 [$CO(CH_2)_2CH_2(CH_2)_2O$], 26.1 [$COCH_2CH_2(CH_2)_3O$], 29.0 [$CO(CH_2)_3CH_2CH_2O$], 34.3 [$COCH_2(CH_2)_4O$], 36.0 [$CH_2CH(COOH)$], 42.3 [br, $CH_2CH(COOH)$], 64.5 [$CO(CH_2)_4CH_2O$], 173.6 [$CO(CH_2)_5O$], 177.8 [$CH_2CHCOOH$] ppm.

**Poly($\epsilon$-caprolactone)-*block*-poly(acrylic acid) (6a).** $n$ = 30, $m$ = 9, and $M_n$ = 4360 ($^1$H NMR). Anal. Calcd for $C_{209}H_{339}O_{79}Br_3$: C, 55.14; H, 7.86. Found: C, 54.89; H, 7.89. TGA in $N_2$: 100−340 °C, 10% mass loss; 340−500 °C, 76% mass loss.

**Poly($\epsilon$-caprolactone)-*block*-poly(acrylic acid) (7b).** $n$ = 121, $m$ = 18, and $M_n$ = 15 300 ($^1$H NMR). DSC: $T_m$ = 59 °C. TGA in $N_2$: 100−350 °C, 4% mass loss; 350−500 °C, 94% mass loss.

**Poly($\epsilon$-caprolactone)-*block*-poly(acrylic acid) (7c).** $n$ = 105, $m$ = 158, and $M_n$ = 25 400 ($^1$H NMR). Anal. Calcd for $C_{1111}H_{1695}O_{528}Br$: C, 56.58; H, 7.26. Found: C, 53.34; H, 6.95. DSC: $T_m$ = 60 °C. TGA in $N_2$: 100−360 °C, 23% mass loss; 360−500 °C, 66% mass loss.

**Poly($\epsilon$-caprolactone)-*block*-poly(acrylic acid) (6b, 7a, and 7d).** The compositions of these polymers are listed in Table 3.

**Formation of Micelles.** Poly($\epsilon$-caprolactone)-*block*-poly(acrylic acid) was first dissolved in a 20:1 THF/water mixture (1.0 mg/mL). An equal volume of nonsolvent for poly($\epsilon$-caprolactone) ($H_2O$) was then added gradually (30.0 mL/h). Usually, micellization occurred when ca. 20−30 vol % water was added. A blue tint appeared, indicating the formation of micelles. The mixture was stirred for ca. 15 h at room temperature, and THF was then removed by dialysis in water for 1 day. The concentration of diblock copolymer was usually 0.3−0.4 mg/mL after removal of THF. Solid-state samples of the micelles were obtained by lyophilization.

**General Procedure for Cross-Linking the PAA Block To Form SCKs.** To the micelle solution of PCL-*b*-PAA was added dropwise an aqueous solution of 1-(3-dimethylaminopropyl)-3-ethylcarbodiimide methiodide. The mixture was stirred for ∼10 min before the aqueous solution of the cross-linker, 2,2′-(ethylenedioxy)bis(ethylamine), was added dropwise. The reaction mixture was allowed to stir overnight at room temperature and then dialyzed against distilled water for 3−4 days to remove byproducts of the cross-linking reaction. The average heights ($H_{av}$) and diameters ($D_{av}$) of SCKs adsorbed onto a mica surface were obtained by tapping-mode AFM. The hydrodynamic diameter ($D_h$) of SCKs in aqueous solution was determined by DLS.

**SCK 8 (50% Cross-Linked).** To the micelle solution of **6b** (0.30 mg/mL, 30 mL, 0.058 mmol of acrylic acid unit) were added 1-(3-dimethylaminopropyl)-3-ethylcarbodiimide methiodide (8.6 mg, 0.029 mmol) and 2,2′-(ethylenedioxy)bis(ethylamine) (2.0 mg/mL, 1.0 mL, 0.014 mmol). $H_{av}$ = 6 ± 1 nm, and $D_{av}$ = 40 ± 6 nm.

**SCK 9 (50% Cross-Linked).** To the micelle solution of **7b** (0.30 mg/mL, 40 mL, 0.014 mmol of acrylic acid unit) were added 1-(3-dimethylaminopropyl)-3-ethylcarbodiimide methiodide (2.1 mg, 0.007 mmol) and 2,2′-(ethylenedioxy)bis(ethylamine) (1.0 mg/mL, 0.6 mL, 0.004 mmol). $H_{av}$ = 20 ± 1 nm, and $D_{av}$ = 109 ± 15 nm.

**SCK 10 (25% Cross-Linked).** To the micelle solution of **7b** (0.24 mg/mL, 20 mL, 0.006 mmol of acrylic acid unit) were added 1-(3-dimethylaminopropyl)-3-ethylcarbodiimide methiodide (0.5 mg, 0.0015 mmol) and 2,2′-(ethylenedioxy)bis(ethylamine) (0.2 mg/mL, 0.5 mL, 0.0008 mmol). $H_{av}$ = 16 ± 2 nm, $D_{av}$ = 83 ± 8 nm, and $D_h$ = 100 ± 1 nm.

**SCK 11 (50% Cross-Linked).** To the micelle solution of **7b** (0.24 mg/mL, 20 mL, 0.006 mmol of acrylic acid unit) were added 1-(3-dimethylaminopropyl)-3-ethylcarbodiimide methiodide (0.9 mg, 0.003 mmol) and 2,2′-(ethylenedioxy)bis(ethylamine) (0.2 mg/mL, 1.0 mL, 0.0015 mmol). $H_{av}$ = 17 ± 3 nm, $D_{av}$ = 105 ± 9 nm, and $D_h$ = 99 ± 1 nm.

**SCK 12 (100% Cross-Linked).** To the micelle solution of **7b** (0.24 mg/mL, 20 mL, 0.006 mmol of acrylic acid unit) were added 1-(3-dimethylaminopropyl)-3-ethylcarbodiimide methiodide (1.8 mg, 0.006 mmol) and 2,2′-(ethylenedioxy)bis(ethylamine) (0.2 mg/mL, 2.0 mL, 0.003 mmol). $H_{av}$ = 18 ± 3 nm, and $D_{av}$ = 172 ± 13 nm. A solid sample of SCK **12** was obtained by lyophilization. DSC: $T_g$ = −62 °C, $T_m$ = 58 °C.

**SCK 13 (100% Cross-Linked).** To the micelle solution of **7c** (0.25 mg/mL, 20 mL, 0.031 mmol acrylic acid unit) were added 1-(3-dimethylaminopropyl)-3-ethylcarbodiimide methiodide (8.9 mg, 0.031 mmol) and 2,2′-(ethylenedioxy)bis(ethylamine) (1.0 mg/mL, 2.2 mL, 0.015 mmol). A bimodal distribution of particle size was observed by both AFM ($H_{av}$ = 8 ± 1 and 15 ± 2 nm, $D_{av}$ = 43 ± 5 and 103 ± 16 nm) and DLS (44 ± 4 and 255 ± 50 nm). The solid sample of SCK **13** was obtained by lyophilization. DSC: $(T_g)_1$ = −67 °C, $(T_g)_2$ = −50 °C, $(T_m)_1$ = 48 °C, $(T_m)_2$ = 56 °C.

**SCK 14 (50% Cross-Linked).** To the micelle solution of **7d** (0.50 mg/mL, 600 mL, 1.9 mmol of acrylic acid unit) were added 1-(3-dimethylaminopropyl)-3-ethylcarbodiimide methiodide (28.5 mg, 0.96 mmol) and 2,2′-(ethylenedioxy)bis(ethylamine) (20 mg/mL, 3.6 mL, 0.48 mmol). $H_{av}$ = 10 ± 1 nm, and $D_{av}$ = 45 ± 6 nm. A solid sample of SCK **14** was obtained by lyophilization. DSC: $T_g$ = −68 °C, $T_m$ = 53 °C.

**Hydrolysis of the PCL Core of the SCKs. Hydrolysis in Acidic Conditions.** To the aqueous solution of SCK **8** (10 mL, 0.3 mg/mL) was added 12 M aqueous HCl (2.5 mL). The mixture was stirred in a 70 °C oil bath for 15 h. The solution was then transferred to a dialysis bag and dialyzed against deionized water for 3 days to remove the excess acid and degradation products. The aqueous solutions of SCK **8** before and after hydrolysis were characterized by tapping-mode AFM.

**Hydrolysis in Basic Conditions.** To the aqueous solution of SCK **14** (70 mL, 0.3 mg/mL) was added NaOH (3 mg, 0.08 mmol) to adjust the pH of the solution to 12. The mixture was stirred at room temperature for 14 days. A 10 mL aliquot of the reaction mixture was then dialyzed against deionized water to remove the excess base and degradation products and subjected to AFM analysis ($H_{av}$ = 6 ± 1 nm, and $D_{av}$ = 123 ± 16 nm). The rest of the reaction mixture (ca. 60 mL) was lyophilized and redissolved in $D_2O$ for $^1$H NMR characterization. A small-molecule degradation product, sodium 6-hydroxylhexanoate, was observed. $^1$H NMR ($D_2O$): $\delta$ 0.98 [m, $NaOOC(CH_2)_2CH_2(CH_2)_2OH$], 1.22 [m, $NaOOCCH_2CH_2CH_2CH_2CH_2OH$], 1.85 [t, $J$ = 6.0 Hz, $NaOOCCH_2(CH_2)_4OH$], 3.25 [t, $J$ = 6.0 Hz, $NaOOC(CH_2)_4CH_2OH$] ppm. The NMR sample was lyophilized again and resuspended in THF-$d_8$. Weak signals were observed in the $^1$H NMR (THF-$d_8$): $\delta$ 1.35 [m, $CO(CH_2)_2CH_2(CH_2)_2O$], 1.61 [m, $COCH_2CH_2CH_2CH_2CH_2O$], 2.28 [t, $J$ = 6.0 Hz, $COCH_2(CH_2)_4O$], 4.02 [t, $J$ = 6.0 Hz, $CO(CH_2)_4CH_2O$)] ppm.

**Acknowledgment.** Financial support from the National Science Foundation (Grants DMR-9458025 and -9974457) and Monsanto Co. is gratefully acknowledged. We extend thanks to Professor Tomasz Kowalewski for valuable instruction and assistance with AFM measurements, and to Mr. Christopher G. Clark, Jr., for the schematic drawings of SCK nanoparticles.

JA993941O